Direct Synthesis and Characterization of Hydrophobic Aluminum-Free Ti−Beta Zeolite

T. Blasco,[†] M. A. Camblor,*[,†] A. Corma,[†] P. Esteve,[†] J. M. Guil,[‡] A. Martínez,[†] J. A. Perdigón-Melón,[‡] and S. Valencia[†]

Instituto de Tecnología Química, UPV-CSIC, Avda. Los Naranjos s/n, 46071 Valencia, Spain, and Instituto de Química Física "Rocasolano", CSIC, Serrano 117, 28006 Madrid, Spain

Received: October 9, 1997[⊗]

Incorporation of Ti into the framework of aluminium-free zeolite Beta has been achieved in F^- medium and has produced hydrophobic selective oxidation catalysts. The Ti−Beta(F) materials have been characterized by X ray diffraction, infrared, Raman, ultraviolet, XANES, EXAFS, ^{29}Si MAS NMR, and ^{1}H→^{29}Si CP MAS NMR spectroscopies, adsorption microcalorimetry, and catalytic testing. At near neutral pH the incorporation of Ti into the framework appears to present an upper limit of ca. 2.3 Ti/uc, beyond which anatase is detected in the calcined materials. However, at higher pH (ca. 11) larger amounts of Ti can be incorporated without anatase formation. After calcination, Ti incorporation in the framework is characterized by an increase in the unit cell volume, the appearance of one Raman band and three infrared bands in the region near 960 cm^{-1} and the presence of a strong absorption band in the 205−220 nm ultraviolet spectrum. By ^{29}Si MAS NMR, ^{1}H→^{29}Si CP MAS NMR, and infrared spectroscopies it is concluded that upon contact with ambient humidity there is no hydrolysis of Si−O−Ti bonds in Ti−Beta zeolites prepared by the fluoride route, while it is probably a major feature of those synthesized in OH^- medium. XANES and EXAFS spectroscopies of calcined dehydrated Ti−Beta zeolites unambiguously demonstrate the tetrahedral coordination of Ti with a Ti−O bond length of ca. 1.80 Å. Upon hydration, the changes in the XANES and EXAFS spectra are consistent with a change in the coordination of Ti to reach a state which depends on the composition and synthesis route and which ranges from a 5-fold coordination for Al-free Ti−Beta synthesized by the F^- method to a highly distorted 6-fold coordination in Ti,Al−Beta synthesized in OH^- medium. Adsorption microcalorimetry experiments show the strict hydrophobic nature of pure SiO_2 zeolite Beta synthesized in F^- medium while evidencing a slight increase in the hydrophilicity of the material upon incorporation of Ti to the framework. This is due to the relatively strong adsorption of precisely one H_2O molecule per Ti site. On the contrary, the materials synthesized in OH^- medium show an enhanced hydrophilicity. Finally, Ti−Beta(F) is an active and selective catalyst for oxidation of organic substrates with H_2O_2. A comparison of the activities and selectivities of Ti−Beta(F), Ti−Beta(OH) and TS-1 in the epoxidation of 1-hexene using acetonitrile and methanol as solvents demonstrates that the major differences between Ti−Beta and TS-1 catalysts are intrinsic to each zeolitic structure. Because of its high hydrophobicity, Ti−Beta(F) catalyst can advantageously replace Ti−Beta(OH) in the epoxidation of substrates, like unsaturated fatty acids or esters, which contain a polar moiety.

Introduction

Selective catalytic oxidation of organic compounds by hydrogen peroxide or organic hydroperoxides over Ti-substituted zeolites has received much attention in the past decade mainly because of two reasons. First, their potential industrial applications as oxidation catalysts could replace current stoichiometric or homogeneously catalyzed processes that generate large amounts of waste residues and/or need to be worked out under severe astringent conditions. Secondly, from a fundamental point of view Ti-containing zeolites show the remarkable property of being highly active catalysts in the epoxidation of olefins with aqueous H_2O_2 in the presence of polar solvents. In contrast, the activity of most homogeneous or heterogeneous catalysts based on transition metal compounds is severely retarded by water and polar solvents, and alkylhydroperoxides are the oxidants of choice.[1] Consequently, much attention has been paid to the study of this new class of materials, but little is known about what gives Ti-zeolites their remarkable properties, which are loosely attributed to the isolation of Ti species in the zeolitic framework.

One of the challenges in this field is to understand why different Ti-zeolites seem to have different catalytic properties, beyond those that can be explained by mere shape selectivity constraints imposed by the size and shape of their channels, even if isolated Ti species were incorporated in all cases into the framework. Notably, the most interesting Ti-zeolites, TS-1[2] and Ti−Beta,[3] exhibit a markedly different behavior, exemplified by their different activity and selectivity dependence on the solvent.[4,5] Differences between the "intrinsic" activity and selectivity of both materials were early attributed to the presence of Al in Ti−Beta,[6] but once the synthesis of Ti−Beta was made possible in the absence of Al,[7,8] the differences between the catalytic behavior of these zeolites persisted. We have very recently developed new methods to synthesize Ti−Beta zeolites with a wide range of chemical compositions and

[†] Instituto de Tecnología Química.
[‡] Instituto de Química Física "Rocasolano".
[⊗] Abstract published in *Advance ACS Abstracts,* December 1, 1997.

S1089-5647(97)03288-4 CCC: $15.00
Published on Web 01/01/1998

physical properties.[7−9] Here we report on the state of Ti in Al-free Ti−Beta zeolite prepared by different routes, the different physicochemical properties of these materials, and the implications of these differences on their catalytic behavior for alkenes epoxidation. We conclude that the main differences observed in the activity and selectivity of TS-1 and Ti−Beta in the epoxidation of alkenes are essentially related to their different crystalline structures and cannot be solely attributed to other parameters as previously suggested (presence of Al, presence of defects, hydrophilicity).

Experimental Section

Synthesis of Ti−Beta. Tetraethylammonium cations (TEA^+) were used as the organic structure-directing agent in all the syntheses. The syntheses were done using either F^- or OH^- anions as mineralizers and in the presence or in the complete absence of Al. Four types of Ti−Beta zeolites were thus synthesized and will be denoted according to its chemical composition (Ti^- or Ti,Al−Beta) and synthetic method used (Beta(F) or Beta(OH)). Unless noted otherwise the crystallization temperature was always 413 K, and PTFE lined stainless steel 60 mL autoclaves were used under tumbling (60 rpm). The autoclaves were removed at different time intervals, and the contents were filtered or centrifuged and extensively washed with distillate water.

Beta(F). Al-free Ti−Beta zeolites were synthesized in F^- medium at near neutral pH 8−9 from gels of composition *x* TiO_2:25 SiO_2:14 TEAOH:8.6 H_2O_2:189 H_2O:14 HF, with *x* in the range 0−2.5. The products obtained had an average crystal size in the range 1−5 μm. Smaller crystal sizes (below 1 μm) were obtained by seeding the gels with the dealuminated zeolite Beta, whose preparation is described below. For pure silica Beta(F) ($x = 0$) an unseeded synthesis was done also at 448 K without rotation, to get a material with a crystal size of ca. 10 μm. To incorporate Al in the zeolite framework by this method (Ti,Al−Beta(F) sample) a starting gel of composition TiO_2:50 SiO_2:0.21 Al_2O_3:28 TEAOH:16.8 H_2O_2:361 H_2O:28.4 HF was used.

Beta(OH). Aluminum-free Ti−Beta was synthesized in basic medium (pH ca. 12) from gels of composition *x* TiO_2:40 SiO_2:22 TEAOH:13.5 H_2O_2:265 H_2O, with *x* in the range 0.33-2. Dealuminated zeolite Beta crystals (see below for preparation) were used as seeds, and crystals smaller than 0.5 μm were obtained. The aluminum-containing material (Ti,Al−Beta(OH) sample) was synthesized from a gel of composition TiO_2:60 SiO_2:0.077 Al_2O_3:32.4 TEAOH:613 H_2O.

Experimental details of the synthesis procedures have been already described elsewhere,[3,7−10] except for the Al-containing Beta(F) series. In this case, the same experimental procedure as in the Al-free syntheses[9] was followed, but metal Al was dissolved in TEAOH and then added to the synthesis gel at the end of the preparation.

Dealuminated Zeolite Beta Seeds. A gel of composition SiO_2: 0.04 Al:0.56 TEAOH:6.5 H_2O was crystallized at 413 K for 72 h, yielding nanocrystalline zeolite Beta with ca. 50 nm average crystal size and a Si/Al ratio of ca. 21. Further details of the synthesis were given elsewhere.[11] The zeolite was dealuminated by treatment at 80 °C during 24 h with HNO_3 (60 %) in a liquid to solid ratio of 60.[12] The final Si/Al ratio of the seeds was higher than 1000. A mass ratio seeds/SiO_2 of 0.029 was used in the syntheses.

Characterization. Phase purity was determined from powder X-ray diffraction (XRD) data recorded in a Philips X'Pert MPD diffractometer equipped with a PW3050 goniometer (Cu Kα radiation, graphite monochromator), provided with a variable divergence slit and working in the fixed irradiated area mode. ^{29}Si MAS NMR spectra were recorded at a ^{29}Si frequency of 79.459 MHz and a spinning rate of 5 kHz on a Varian VXR 400S WB spectrometer. Bloch decay (BD) spectra were acquired with a 38.6° pulse length of 3.0 μs and a recycle delay of 20 s. ^{1}H→^{29}Si CP MAS NMR spectra were acquired with a 90° pulse length of 7 μs, contact times of 500, 1500, and 2500 μs, and a recycle delay of 3 s. The ^{29}Si chemical shifts are reported relative to TMS.

Infrared spectra in the region of framework vibrations (1900−300 cm^{-1}) were obtained in a Nicolet 710 FTIR spectrometer using the KBr pellet technique. Spectra in the hydroxyl stretching region (4000−3000 cm^{-1}) were recorded in a BioRad STS 40A FTIR spectrometer using self-supported wafers of 10 mg cm^{-2} outgassed overnight at 673 K and 10^{-3} Pa. Raman spectra in the 1400−150 cm^{-1} region were recorded in a FT-Raman II Bio-Rad spectrometer using a Nd:YAG laser beam (1064 nm). For the detection of anatase (main band at 144 cm^{-1}) additional Raman spectra down to about 50 cm^{-1} were recorded using a DILOR XY spectrometer operating in the micro-Raman mode with the 514 nm line of an Ar laser beam. Diffuse reflectance ultraviolet−visible (DRUV) spectra were recorded in a Cary 5 Varian spectrometer equipped with a "Praying Mantis" cell from Harrick.

X-ray absorption experiments were performed on stations XAS-2 and XAS-3 at LURE (Orsay, France). The X-ray beam was emitted by the DCI ring with a stored current between 228 and 320 mA. The data were collected using Si(311) and Si-(111) two-crystal monochromators for XANES and EXAFS, respectively. At the XAS-2 station the beamline was equipped with two parallel mirrors for harmonic rejection. At the XAS-3 station harmonics were rejected by detuning the monochromator by 50% from the maximum intensity. The spectra were recorded at room temperature in the transmission mode, and the detection was carried out by using two ionization chambers. The samples and the anatase were used as self-supported wafers. The calcined samples were dehydrated at 623 K for 1 h, transferred into a special chamber under Ar atmosphere, and kept under vacuum during the spectra acquisition. Experimental data were analyzed with a set of programs developed by Michalowicz.[13] XANES spectra were treated by subtracting the linear background determined by least-squares fitting of the preedge region and normalized with respect to the beginning of the EXAFS oscillations. The standard procedures for background removal, extraction of EXAFS oscillations, and normalization of the edge absorption were applied. The K^3 weighted Fourier transform between 2.80 and 11.50 $Å^{-1}$ was calculated using a Kaiser window. Filtering of the first peak between 1.09 and 1.96 Å for calcined dehydrated Ti−Beta and between 1.10 and 1.86 Å for rehydrated samples was applied to analyze the first coordination shell of Ti. The EXAFS spectrum of anatase was used as a reference to obtain the phase shift and backscattering amplitude for Ti−O. These functions were calculated considering six oxygen atoms at a distance of 1.95 Å and a Debye−Waller factor $\sigma^2 = 2.9 \times 10^{-3}$ for anatase. The later value was obtained from the simulation of the experimental spectrum using the theoretical curves calculated by Mckale et al.[14]

For adsorption microcalorimetry experiments toluene, *n*-hexane, and water (purity > 99%) were used as adsorbates after purification by successive freeze−thaw cycles inside the adsorption apparatus. Adsorption measurements were performed in a conventional volumetric apparatus.[15] A heat-flow microcalo-

rimeter of the Tian-Calvet type (model BT, Setaram, France) was used to determine differential heats of adsorption by measuring the heat evolved in the adsorption of a given amount of adsorbate. For this purpose the calorimeter cells are part of the volumetric apparatus. The heat/voltage proportionality constant of the microcalorimeter was calibrated by the Joule effect. The correction for the heat evolved in the gas compression associated with the gas entrance in the cell was determined by previous experiments with helium. Before each adsorption experiment the sample was heated in oxygen flow, ca. 30 cm^3/min, increasing the temperature at 4 K/min from room temperature up to 723 K, kept at this temperature for 2 h, and outgassed overnight at the same temperature in a vacuum of more than 1 mPa. Volumetric and calorimetric isotherms were determined simultaneously in the usual way by measuring amounts adsorbed in successive doses at increasing pressures. Experiments were carried out at 315 K. In a different set of experiments water was adsorbed following toluene adsorption after outgassing for 30 min at the temperature of the experiment. The amount of adsorbate removed in the intermediate outgassing was calculated from the desorption calorimetric peak. Amounts adsorbed are expressed as millimole of adsorbate per gram of sample dried under vacuum at 723 K.

Catalytic Activity. The experiments of epoxidation of 1-hexene were performed in a 25 mL round-bottom flask immersed in a thermostated bath and equipped with a condenser, a thermometer, and a magnetic stirrer. Typically, 17 mmol of alkene, 11.8 g of solvent (either methanol or acetonitrile), and 0.4 g of diluted H_2O_2 (35 wt % in water) were homogenized in the flask under stirring, and the mixture was heated at 323 K. Then, 0.1 g of catalyst was added at once to the reaction mixture (time zero). Small aliquots were carefully withdrawn from the mixture at time intervals to follow the kinetics of the reaction. For the epoxidation of oleic acid, 1 mmol of alkene, 2 mL of acetonitrile (solvent), 24 mg of H_2O_2 (35 wt % in water), and 30 mg of catalyst were mixed in a 5 mL flask and heated up to 323 K under continuous stirring. In both cases the reaction products were analyzed by gas chromatography in a Varian 3400 GC equipped with a capillary column (5% methylphenylsilicone, 25 m length) and a FID. Product identification was performed by GC−MS and available standard compounds. Unreacted hydrogen peroxide was determined by iodometric titration.

Results and Discussion

Synthesis in Fluoride Medium. In the synthesis of Ti−Beta(F) and Ti,Al−Beta(F) under the conditions described above, no competition of other crystalline phases was detected by powder XRD. However, there is spectroscopic evidence of the presence of anatase in the calcined solids for Ti contents higher than 5 wt % as TiO_2 and final pH of the reaction smaller than ca. 11 (see below). The introduction of Ti in a nearly neutral or slightly basic pure silica reaction mixture in fluoride medium results in a significant increase of the crystallization time and only 50% of the Ti initially present in the reaction mixture is incorporated into the final material, contrarily to the observed behavior in OH^- medium, in which total incorporation is achieved (Figure 1). This holds until a Ti/(Ti + Si) molar fraction in the gel of about 0.06 is reached; beyond this limit, which corresponds in the zeolite to about a 0.037 molar ratio (2.3 Ti/uc), anatase coprecipitates (see below) and the amount of Ti in the solid largely increases (Figure 1).

It is interesting that the yield (and the apparent upper limit) of Ti incorporation into the framework of zeolite Beta in fluoride medium at nearly neutral pH is much lower than that obtained

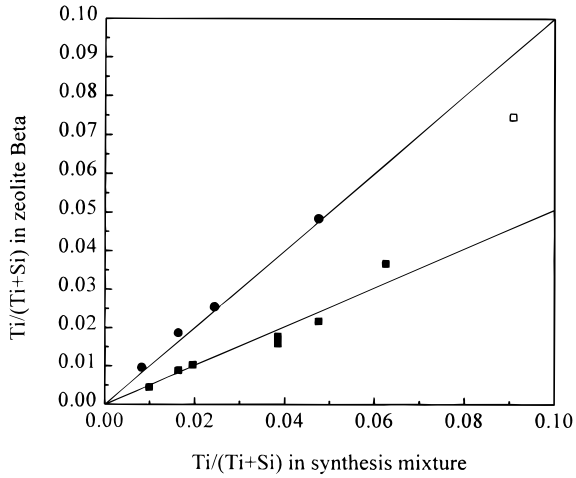

Figure 1. Efficiency of the incorporation of Ti to the zeolite Beta structure for synthesis in OH- medium (●) and in F^- medium at pH = 7−9 (■). The open square corresponds to a calcined material in which a large amount of anatase was detected.

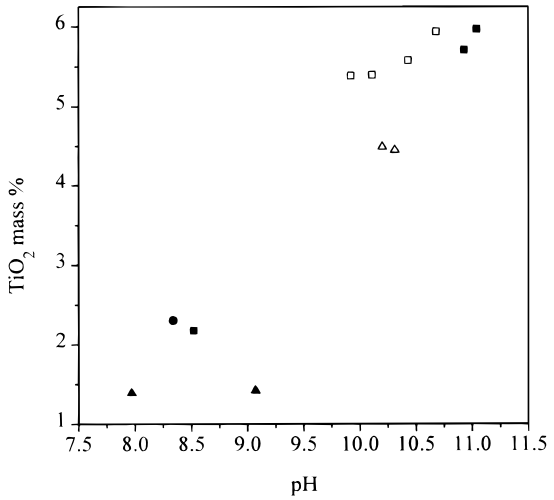

Figure 2. Incorporation of Ti to the solids as a function of synthesis pH and F^- concentration. F^-/SiO_2 = 0.40 (●), 0.54 (■), and 1.08 (▲). Open symbols correspond to materials in which anatase was detected.

when OH^- anions are used as mineralizers (Figure 1). Obviously, the differences between both types of synthesis (F^- *vs* OH^-) are the pH and the presence of F^-. To check the influence of both parameters on Ti incorporation, we performed a series of experiments in which F^-/Si ratio and pH were varied by using different amounts of HF, NH_4F, TEAOH, and HCl. The results are shown in Figure 2. The amount of Ti in the final solids strongly depends on the pH of the reaction mixture. At a pH beyond 10 all Ti initially present in the reaction mixture is found in the final solid, but anatase is generally detected in the calcined product. However, a further pH increase to about 11 avoided anatase precipitation, preserving the complete incorporation of Ti. This is also the common observation in the synthesis of Ti−Beta in OH^- medium (pH ca. 12). The effect of F^- on the final yield of Ti is also clear, though less marked: an increase in F^- concentration at a given pH causes a decrease in the amount of Ti recovered. These results suggest that, in the absence of alkali cations, the formation of soluble titanosilicate species is favored at high pH, affording total Ti incorporation into the framework of zeolite Beta. At low pH soluble complexes with F^- exist that maintain a significant portion of Ti in solution, precluding total incorporation to the zeolite. Apparently, such complexes are less stable as pH increases and,

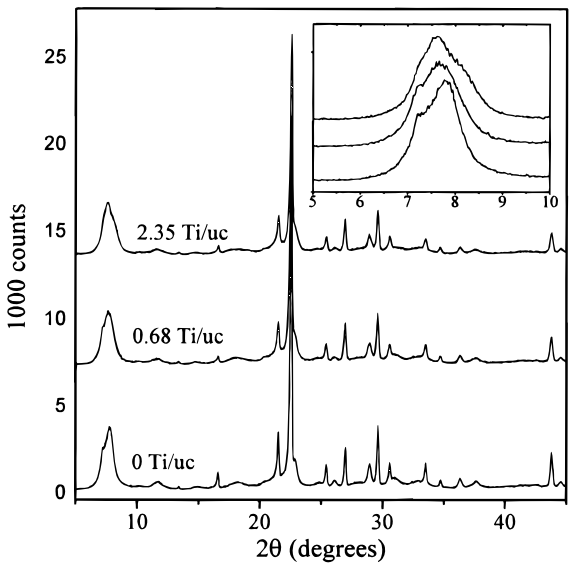

Figure 3. X-ray diffraction patterns of aluminum-free zeolite Beta samples synthesized by the fluoride route with different Ti contents. A gradual change of the shape of the low-angle peak as the Ti content increases, possibly indicating symmetry changes or variations in the relative proportions of polymorphs,[17] is shown in the inset.

as a consequence, at an intermediate pH total recovery of Ti in the solids (or almost total, depending on F^- concentration) but only partial incorporation in the framework occurs. Figure 2 demonstrates that the incorporation of Ti in the framework of zeolite Beta in F^- medium strongly depends on the pH. For this reason, we have not found so far an "intrinsic" upper limit for the isomorphous substitution of Si by Ti.

Evidence for the Isomorphous Substitution. The isomorphous substitution of Si by Ti in zeolites can be ascertained by a combination of physicochemical techniques and catalytic tests. One of the most widely used techniques is powder X-ray diffraction, where the incorporation of Ti in the framework is, in principle, expected to cause a linear increase in the unit cell volume, due to the longer Ti−O bond distance (1.79−1.92 Å, depending on the actual coordination number of Ti) compared to the Si−O bond distance (typically 1.60−1.65 Å in zeolites). Although it has been recently shown that isomorphous substitutions in zeolites do not necessarily bear the expected trend in unit cell expansions or contractions,[16] all reports on Ti-zeolites have shown so far the expected increase in unit cell volume. For zeolite Beta this technique is much limited by the structural nature of the material, which is an intergrowth of at least two polymorphs.[17] Probably due to that, but maybe also due to possible symmetry changes originated by the isomorphous substitution, we were able to index the XRD patterns of the Ti−Beta(F) calcined materials only with the indices of the tetragonal polymorph A. Actually, the XRD patterns of zeolite Beta samples synthesized by the fluoride route show a gradual change in the shape of the first low angle peak as the Ti content increases (Figure 3). The shape of this peak is sensitive to changes in the relative proportion of different polymorphs.[17] Thus, this could indicate a decreased presence of polymorph A as the Ti content increases but symmetry changes could also be responsible for that effect.

As shown in Figure 4, there is a linear increase in the unit cell volume of polymorph A as the Ti content of the material synthesized at pH = 7−9.5 (see above) increases up to a Ti/(Ti + Si) mole fraction in the zeolite of 0.037. Beyond this value no further increase of the unit cell volume occurs and anatase starts to show up in the DRUV and Raman spectra (see

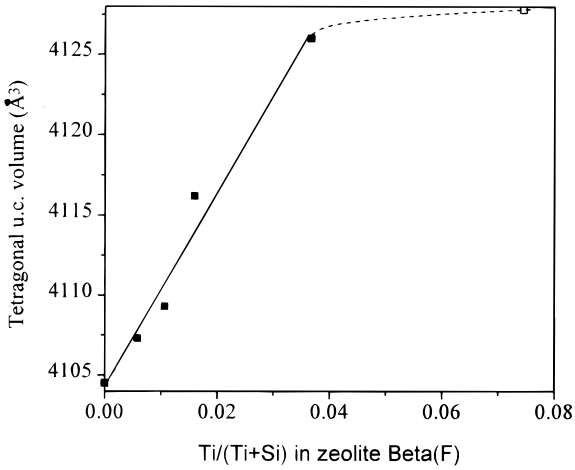

Figure 4. Variation of the unit cell volume of Ti−Beta(F) calcined materials synthesized at near neutral pH, indexed according to the tetragonal polymorph A,[17] as a function of their Ti content. (The open square corresponds to a sample containing a large amount of anatase.)

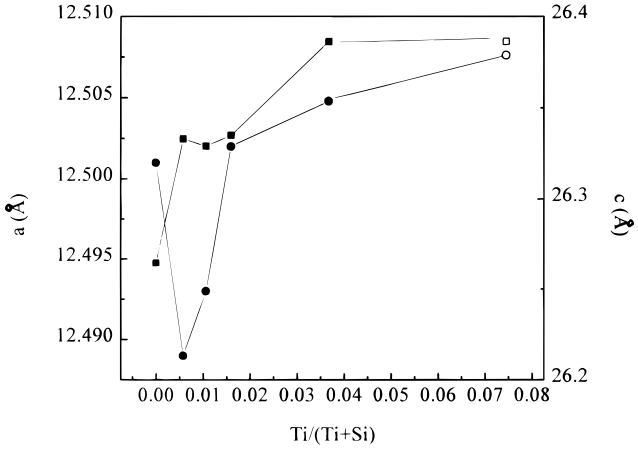

Figure 5. Change in the tetragonal unit cell parameters (●, *a*; ■, *c*) of Ti−Beta(F) calcined materials as a function of Ti content (open symbols correspond to a material containing a large amount of anatase).

below). As shown in Figure 5, the expansion of the unit cell upon the isomorphous substitution is markedly anisotropic, occurring in a larger extent for parameter *c*, whereas parameter *a* shows a minimum at low Ti content.

The incorporation of Ti in the zeolite Beta framework in F^- medium is also evidenced by spectroscopic techniques. First, all calcined Beta(F) samples show a sharp absorption in the 205-220 nm ultraviolet region (Figure 6), with no absorptions attributable to anatase when the Ti molar fraction in the material is below 0.037 (2.3 Ti/uc). Beyond that concentration, anatase starts to show up in the materials synthesized at nearly neutral pH, as evidenced by the presence of a broad absorption band around 330 nm. For materials synthesized at higher pH (above ca. 11) no anatase is detected by DRUV despite its high Ti content. Secondly, Ti−Beta(F) samples also show absorptions in the 950-980 cm^{-1} region of the infrared (Figure 7) and Raman (Figure 8) spectra which are generally attributed to the presence of Ti in the framework, although the assignment of such bands is still a matter of debate (see below). Finally, the Raman spectra in the low Raman shift region (Figure 9) show that no anatase (characterized by a strong adsorption at ca. 144 cm^{-1}) is formed when the Ti molar fraction in the material synthesized at nearly neutral pH is below the upper limit mentioned above. Additional spectroscopic and catalytic proofs of the isomorphous substitution of Si by Ti are discussed below.

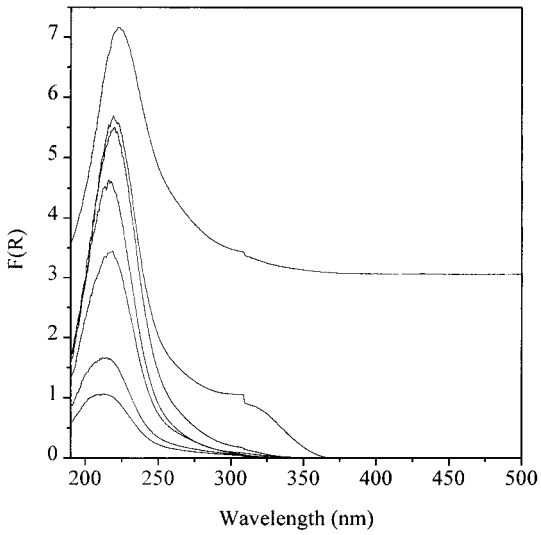

Figure 6. Diffuse reflectance ultraviolet spectra of calcined Ti−Beta samples synthesized in F^- medium at near neutral pH (from bottom to top: 0.37, 0.68, 1.05, 2.35, 1.38, 4.77 Ti/uc) and at pH ≈ 11 (2.87 Ti/uc, vertically offset for clarity).

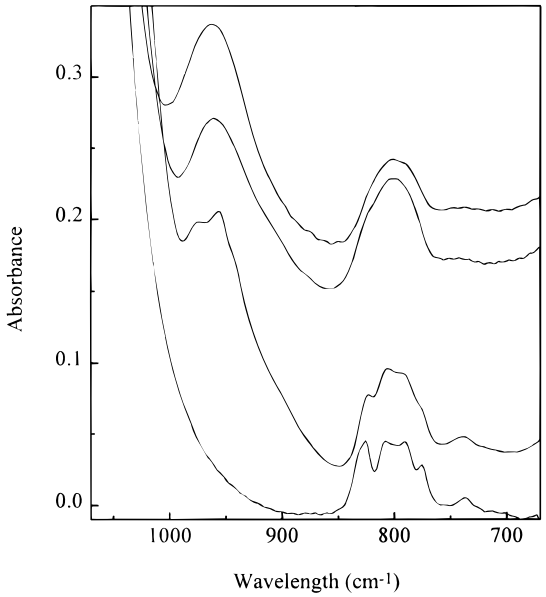

Figure 7. Infrared spectra of calcined zeolite Beta materials: (bottom to top) pure silica(F), Ti−Beta(F, 1.03 Ti/uc), high silica(OH, Si/Al>700), and Ti−Beta(OH, 1.63 Ti/uc).

^{29}Si MAS NMR Spectroscopy. We have previously shown that pure silica zeolite Beta synthesized in fluoride medium in the presence of TEA^+ is free of connectivity defects, within the detection limits of BD and CP ^{29}Si MAS NMR spectroscopies.[18] By the CP technique, however, it is possible to detect Si−OH groups in the external surface, provided that the crystallites are small enough (<ca. 10 μm, see Figure 10). The absence of connectivity defects brings about a high local order in pure silica Beta and a lack of dipolar coupling to protons that allow sharp lines and a remarkable high resolution of Si(4Si) crystallographic sites in the ^{29}Si MAS NMR spectrum of the calcined sample. When Ti is incorporated to Al-free zeolite Beta by the route described here, a broadening of the peaks is apparent in the ^{29}Si BD MAS NMR spectrum (Figure 11). This broadening, which increases as the Ti content increases, causes a major loss of resolution, and only three broad resonances are evident at ca. −112, −113, and −116 ppm. A similar broadening was observed in MFI materials when Si is substituted

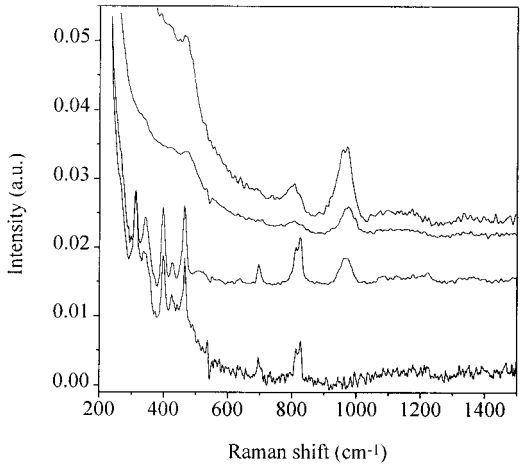

Figure 8. Raman spectra of calcined materials: (bottom to top) pure silica Beta(F), Ti−Beta(F, 1.05 Ti/uc), Ti−Beta(OH, 1.63 Ti/uc), and Ti,Al−Beta(OH, 2.32 Ti/uc, 0.50 Al/uc).

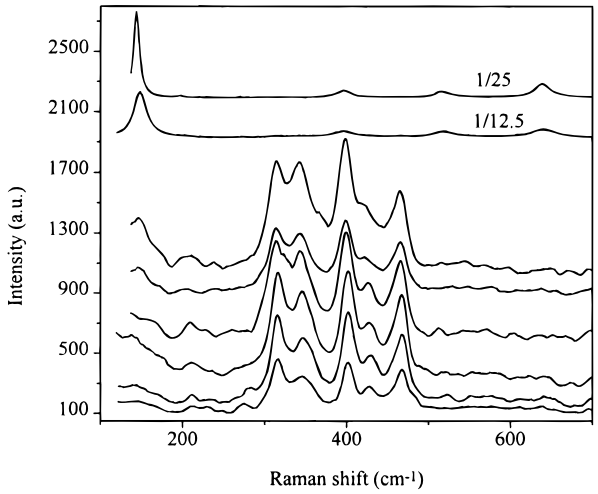

Figure 9. Raman spectra in the low Raman shift region of (bottom to top) silica Beta(F) and Ti−Beta(F) (0.37, 0.68, 1.02, 1.38, 2.35, and 4.77 Ti/uc) calcined samples and anatase.

by either Ti[19] or Ge.[20] The reason for this is most likely a decreased local order due to the distortion of the framework caused by the incorporation of Ti atoms and the presence of overlapping $Si(OSi)_4$ and $Si(OSi)_3OTi$ resonances unspecifically occupying different crystallographic sites. Another plausible explanation for this loss of resolution could be the presence of a high concentration of connectivity defects, which could arise from the hydrolysis of Si−O−Ti bonds. However, this is not the case for Ti−Beta(F), as no Q^3 bands are detected in the BD ^{29}Si NMR (Figure 11). More conclusively, ^{1}H→^{29}Si cross polarization experiments, which are more sensitive to Si−OH groups, reveal the presence of only a small concentration of such moieties in these materials, and this concentration appears to be dependent on crystal size but not on Ti concentration (Figure 10). Therefore, we assign these bands to Si−OH moieties at the external surface of the crystallites. Finally, the increase in water content of the zeolites as Ti content increases (due to the increase in hydrophilicity, see below) could also contribute to the loss of resolution by broadening of the ^{29}Si MAS NMR lines through dipolar coupling with water protons. However, ^{1}H decoupled ^{29}Si MAS NMR experiments (not shown) demonstrate this has only a minor broadening effect.

Contrarily to these observations, the ^{29}Si MAS NMR spectrum of Ti−Beta(OH) clearly evidences the presence of a high concentration of Si−OH defect groups. In the BD experiments

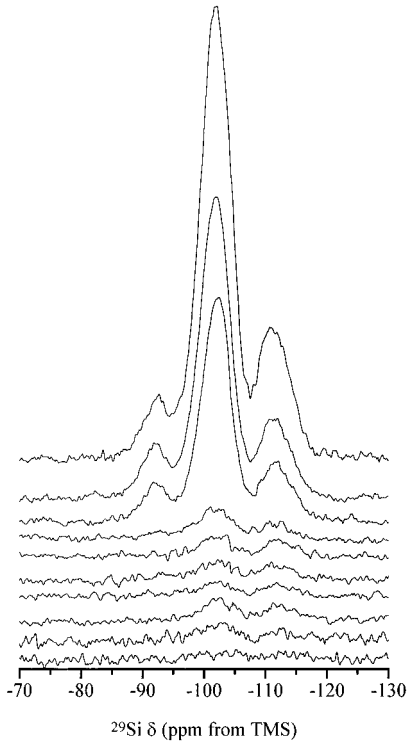

Figure 10. ^{29}Si CP MAS NMR spectra of calcined Beta samples (contact time: 1500 μs). Bottom to top: pure silica Beta(F) with approximate crystal size of 10, 3, and 0.5 μm; Ti−Beta(F) of about 3 μm (0.57 and 1.03 Ti/uc); Ti−Beta(F) of less than 1 μm (0.66 and 2.35 Ti/uc); Ti−Beta(OH) of less than 0.5 μm (0.69, 1.35, and 1.63 Ti/uc). All the spectra are plotted in absolute intensity scale.

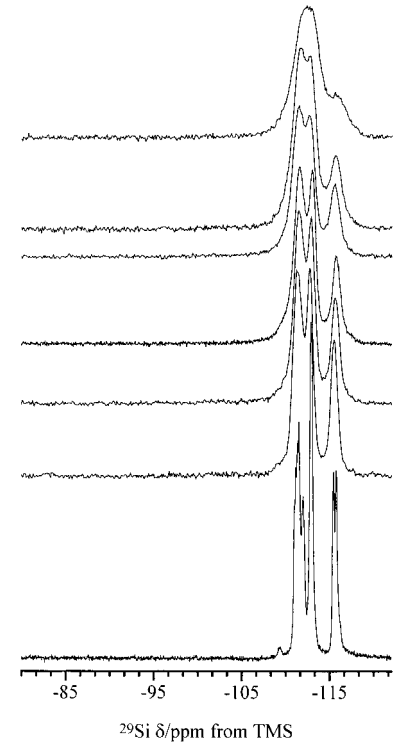

Figure 11. ^{29}Si BD MAS NMR spectra of Al-free zeolite Beta materials synthesized in F^- medium: (bottom to top) pure silica Beta and Ti−Beta with 0.37, 0.66, 1.03, 1.05, 1.38, and 2.35 Ti/uc. Note the absence of any resonance at fields below −109 ppm.

(Figure 12) an increased broadening of the Si(4Si) resonances, with a concomitant higher loss of resolution when compared to Ti−Beta(F) materials is apparent. Furthermore, the presence

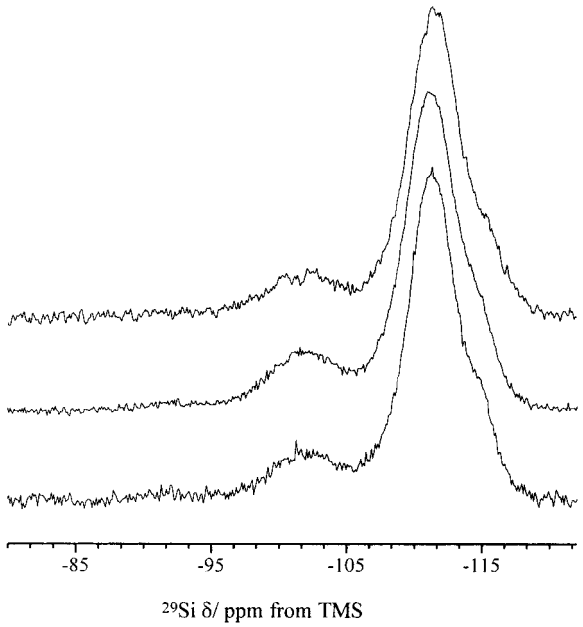

Figure 12. ^{29}Si BD MAS NMR spectra of Al-free zeolite Beta materials synthesized in OH^- medium: (bottom to top) 0.69, 1.35, and 1.63 Ti/uc. Note the presence of a band at ca. −102 ppm, assigned to Q^3 species, and a small band at ca. −92 ppm, assigned to Q^2 species.

SCHEME 1

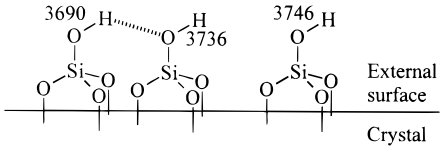

of Si(3Si,1OH) at ca. −102 ppm, that is, Q^3 species in connectivity defects, already seen in the Bloch decay spectrum, is clearly demonstrated under ^{1}H→^{29}Si cross polarization conditions (Figure 10) which evidence even the presence of some Si(2Si,2OH) Q^2 signals at ca. −92 ppm. Apparently, the concentration of such moieties does depend on the Ti content in Ti−Beta(OH) materials and can thus be related in part to the hydrolysis of Si−O−Ti bonds.

FTIR Spectroscopy. *OH Stretching Region (3200−4000* cm^{-1}*).* The investigation of this region of the spectrum is limited to some extent by the necessity to grind the powders to make self-supported wafers. This causes some breaking of the crystallites and therefore the formation of terminal Si−OH groups in all the samples, thus diminishing the differences between them and precluding the extraction of quantitative information. Notwithstanding we can see that pure silica Beta-(F) samples display only small and relatively narrow bands in the 3650−3750 cm^{-1} region (Figure 13). Because of their narrowness and their position, and based on the ^{1}H→^{29}Si CP MAS NMR mentioned commented above, all three bands (3690, 3736, 3746 cm^{-1}) are assigned to terminal Si−OH groups. The difference in wavenumbers is primarily related to the silanol groups being involved or not in weak hydrogen bonding. Thus, the band at 3746 cm^{-1} is assigned to free Si−OH groups,[21] that at 3736 cm^{-1} is assigned to those Si−OH groups in which the O is weakly hydrogen bonded to an adjacent OH moiety, which itself is considered to be responsible of the band at around 3690 cm^{-1} (Scheme 1). It is known that hydrogen bonding causes the OH stretching bands to shift to lower wavenumbers and to broaden, the magnitude of both effects being related to the strength of the hydrogen bond. Thus, the relatively narrow band at 3690 cm^{-1} cannot be due to an OH involved in a very

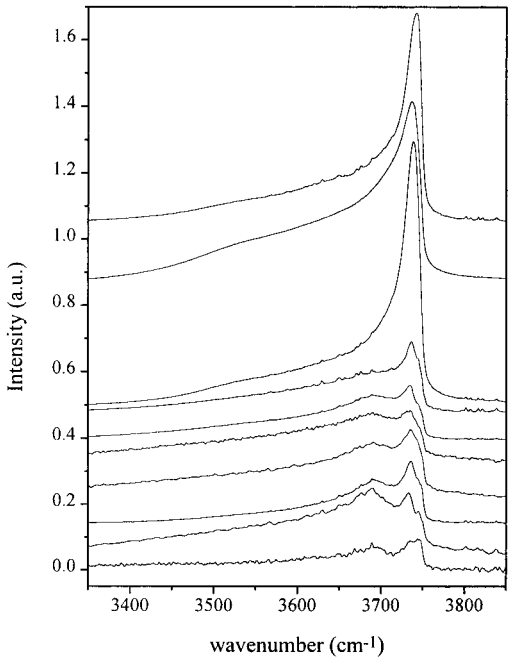

Figure 13. FTIR spectra of calcined dehydrated Beta samples in the OH stretching region: (bottom to top) pure SiO_2 Beta(F) (crystal size of about 10, 3 and 0.5 μm); Ti−Beta(F) of about 3 μm (0.57 and 1.03 Ti/uc); Ti−Beta(F) of less than 1 μm (0.68 and 2.35 Ti/uc); Ti−Beta-(OH) of less than 0.5 μm (0.69, 1.35, and 1.63 Ti/uc). A fraction of the OH observed correspond to Si−OH groups formed upon breaking the crystallites by grinding before making the self-supported wafers (see text).

strong hydrogen bond (which in zeolites typically yield very broad bands covering the 3400−3700 cm^{-1} region), and we propose it is due to a terminal Si−OH group involved in a hydrogen bond which, because of the geometry imposed by the crystal surface, must deviate strongly from the linearity and thus has to be weak (Scheme 1). For the reasons given above (necessity to grind the samples), a clear correlation between the crystal size and the intensity of these bands is not observed.

In the case of Ti−Beta(F) samples, the same three bands with roughly the same intensities as in pure silica Beta(F) are observed (Figure 13). No changes due to crystal size or Ti content are apparent, and the bands are ascribed, as above, to terminal Si−OH groups in the external surface of the crystallites. We conclude that no hydrolysis of Si−O−Ti bonds has occurred in these samples, in agreement with the $^{1}H \rightarrow {}^{29}Si$ CP MAS NMR results discussed above. In the spectra of Ti−Beta(OH) samples (Figure 13) one sharp and intense band at around 3739 cm^{-1} and a weak and very broad band in the 3400−3700 cm^{-1} region are observed and assigned to free Si−OH groups and Si−OH groups involved in strong hydrogen bonds, respectively. The major differences when compared to Beta(F) samples are likely due to the presence of a large concentration of defects in the Beta(OH) samples. It is well-known that high-silica zeolites synthesized in OH- medium show a large concentration of connectivity defects, typically exceeding the concentration needed to counterbalance the template charges.[22] In Ti−Beta-(OH) samples, although there seems to be an increase in intensity when the Ti content increases for the broad band at around 3500 cm^{-1}, we will not draw any conclusion based on this, due to the dependence of the intensity of hydrogen-bonded OH groups on the strength of the hydrogen bond.

Framework Vibrations Region (300−1300 cm^{-1}). Very interestingly, Beta(F) zeolites distinctly show three absorptions bands in the 960 cm^{-1} infrared region (Figure 7), whereas

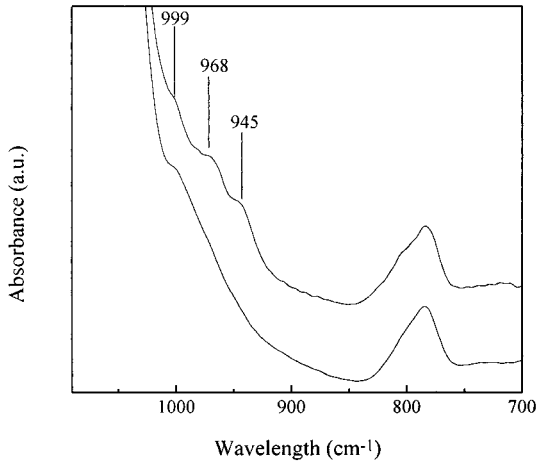

Figure 14. Infrared spectra in the 960 cm^{-1} region of as-made Ti−Beta(F, 2.87 Ti/uc, top) and Ti−Beta(OH, 1.63 Ti/uc, bottom).

typically Ti-zeolites synthesized in OH^- medium show just a broad band, possibly due to the large concentration of Si−OH defect groups present in these samples.

In light of the previous results (negligible hydrolysis of Si−O−Ti bonds in Ti−Beta(F)) it is worth considering the origin of the infrared absorptions near 960 cm^{-1}, characteristic of Ti-zeolites. This band was early attributed to a Si−O stretching vibration in Si−O−Ti groups,[23] and later to a titanyl Ti═O group.[24] We assigned[25] it to the $Si-O^-$ bond in defects because in the as-made TS-1 and Ti−Beta zeolites the infrared spectra show two shoulders, the first one at 1014 cm^{-1} in TS-1 (assigned to $Si-O^-TPA^+$) and 999 cm^{-1} in Ti−Beta (assigned to $Si-O^-TEA^+$) and the second one near 970 cm^{-1} (assigned to $Si-O^-H^+$). Calcination yield in both cases a single, stronger band near 960 cm^{-1} ($Si-O^-H^+$). By a partial solid state exchange of calcined Ti−Beta with TEABr, the original spectrum is restored in part (shoulders at 999 and ≈960 cm^{-1}).[25] Thus, the relatively strong absorption band ca. 960 cm^{-1}, which appears to be characteristic not only of Ti-containing zeolites but also of zeolites containing other metals (V, Cr, Sn, ...)[26] and even high silica zeolites containing a high concentration of connectivity defects (see Figure 7), was assigned in Ti−Beta and TS-1 to $Si-O^- H^+$ defects promoted by the hydrolysis of Ti−O−Si bonds. However, we have now demonstrated that in Ti−Beta(F) there is no noticeable hydrolysis of Ti−O−Si bonds, and therefore the absorption bands near 960 cm^{-1} cannot be due to Si−OH defects, which are practically absent in these zeolites. Thus, the stretching of Si−O bonds in Si−O−Ti groups appears to be the major contribution to the absorption in this region in Ti-zeolites, in agreement with previously reported experimental results.[27] The reason for three different components, which are only resolved in the absence of a significant concentration of Si−OH groups, is not presently understood.

We believe however that Si−OH defect groups can also have a contribution to the 960 cm^{-1} band in Ti−Beta(OH) and other metal-containing zeolites synthesized in OH^- medium, causing a lower resolution in their spectra. Finally, it is important to point out that the as-made Ti−Beta(F) materials show an infrared spectrum in this region very similar to that already reported for as-made Ti,Al−Beta(OH) samples (Figure 14): there are three shoulders at ca. 999, 970, and 950 cm^{-1} rather than a strong absorption band. While the difference between calcined and as-made materials can be likely related to the different coordination of Ti before and after calcination, as

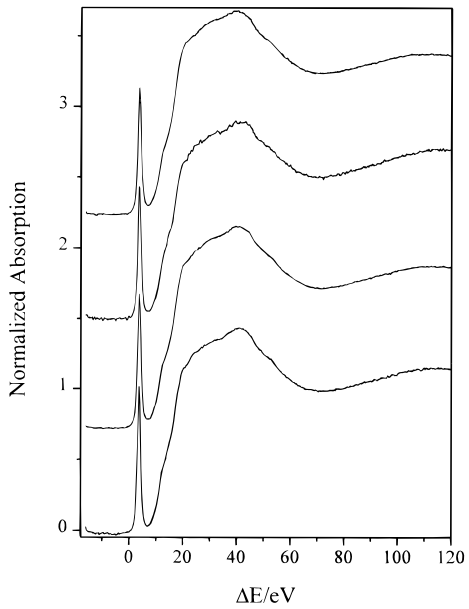

Figure 15. XANES spectra of calcined dehydrated samples. From bottom to top: Ti−Beta(F, 1.05 Ti/uc), Ti−Beta(OH, 1.63 Ti/uc), Ti,-Al−Beta(F, 0.73 Ti/uc, 0.54 Al/uc) and Ti,Al−Beta(OH, 2.32 Ti/uc, 0.50 Al/uc).

evidenced by XANES spectroscopy (see below), we presently lack a full understanding of the infrared spectra of Ti-zeolites.

X-ray Absorption Spectroscopy. Information on the local geometry of Ti can be gathered from X-ray absorption spectra of Ti-zeolites in the Ti K-edge region. Typically, Ti in a distorted octahedral environment presents three preedge peaks of low intensity, the intensity of the central peak (corresponding to $1s \rightarrow t_{2g}$ electronic transitions) increasing with the distortion of the octahedral site. The position of the central transition, relative to the first inflection point of Ti metal, is typically about 5.5 eV in oxides and about 4.8 eV in silicates. On the contrary, Ti in 4- or 5-fold coordination presents a single intense preedge peak (corresponding to the allowed $1s \rightarrow t_2$ electronic transition for tetrahedral symmetry) shifted to lower energy with respect to the central peak in octahedral sites (4.0-4.5 eV for square pyramidal sites and around 3.5 eV for tetrahedral sites).

Calcined Dehydrated Samples. The Ti K-edge XANES spectra of four Ti−Beta samples representative of the four types of materials (Ti−Beta(F), Ti−Beta(OH), Ti,Al−Beta(F), and Ti,Al−Beta(OH)) after calcination and dehydration are given in Figure 15. All of them consist of one sharp and strong preedge peak with small differences in their intensities (Table 1). Only for Ti−Beta(F) is the enhanced prepeak intensity noticeable when compared with the other samples and other reported Ti zeolites.[28−31] The peak intensity and energy position clearly indicate the tetrahedral coordination of Ti.[32−34] Previous publications[30] have reported that the prepeak becomes less intense and wider and is shifted to higher energy when octahedral Ti is present in the form of extraframework anatase or in systems with significant disorder in Ti−O distances and Ti−O−Si angles. According to these considerations, the small value of the full width at half-maximum allows us to discard the existence of significant amounts of Ti in higher coordination and suggest the uniformity of the tetrahedral Ti species in the Ti−Beta samples studied here. All the preedge spectral features shown in Table 1 are then consistent with the insertion of Ti into the zeolite Beta framework.

For all the dehydrated Beta samples the coordination number is consistent, within experimental error, with a tetrahedral coordination. This is further confirmed by the Ti−O interatomic distance, characteristic of this geometry[35] and similar to those previously reported for calcined dehydrated Ti−Beta[31] and TS-1.[30,31] The Debye−Waller factors are in all cases smaller than that of anatase, indicating that the Ti−O distances of the four bonds are quite similar. Indeed this result is not unusual for tetrahedral Ti compounds.[31,34,36]

Calcined Rehydrated Samples. The Ti K-edge XANES spectra obtained after exposure of the Ti−Beta samples to ambient humidity are shown in Figure 16, and the spectral characteristics listed in Table 1. In this case, remarkable differences are observed among the Ti−Beta samples. Rehydration of Ti−Beta(F) produces a minor decrease and broadening of the prepeak, which remains quite strong and sharp. The effects of rehydration are more noticeable for the samples synthesized in OH medium, especially for Ti,Al−Beta(OH) (Figure 16, Table 1). A deep change is observed for this sample as the prepeak strongly decreases, becomes broader, and shifts to higher energy (Figure 16, Table 1) compared to the same sample in the dehydrated state. Since these differences cannot be due to the presence of different amounts of extraframework anatase, the results shown in Figure 16 suggest that the degree of interaction of Ti with water is strongly affected by the hydrophobic/hydrophilic character of the zeolitic framework. The XANES spectra of hydrated Ti−Beta(F) and Ti,Al−Beta-(F) are consistent with the presence of Ti in either 4-fold or 5-fold coordination. The adsorption measurements (see below) indicate a strong adsorption of one water molecule per Ti and accordingly the changes observed after rehydration can be interpreted as due to the insertion of one water molecule in the coordination sphere of Ti to become penta-coordinated. The XANES spectrum of Ti,Al−Beta(OH) displays a relatively small and broad prepeak with a shoulder on the left side, indicating that Ti is mainly in a highly distorted octahedral symmetry, and, then, that two water molecules are coordinated to each framework Ti atom. Probably, a mixture of 5-fold- and 6-fold-coordinated Ti is present in Ti−Beta(OH). The results shown in Figure 16 suggest that as the water affinity (hydrophilicity) of the zeolitic network progressively increases, additional water molecules can enter the coordination shell of Ti.

Although in the most extended interpretation of the XANES spectra of Ti-containing zeolites the changes observed upon hydration are ascribed to coordination of framework Ti to water,[28−30,33] an alternative explanation is the distortion of the parent tetrahedral symmetry due to the hydrolysis of the Ti−O−Si bridges to give tetrahedral Ti sites of the $[OHTi(OSi)_3]$ type and sylanols.[29,30] The presence of $[OHTi(OSi)_3]$ and $[Ti(OSi)_4]$ species has been recently suggested for calcined dehydrated TS-1, the former type being predominant at low Ti concentrations.[36] The formation of $[OHTi(SiO)_3]$ and $[(OH)_2Ti(OSi)_2]$ species has also been predicted to occur in Ti-substituted zeolites on the basis of computational model calculations, provided that there exists the possibility to stabilize by hydrogen bonding the Si−OH groups formed upon hydrolysis (see below).[37] However, the NMR and IR results presented above indicate that hydrolysis of Ti−O−Si bonds is not a significant event in Ti−Beta(F), while it is probably important in Ti−Beta(OH) samples.

Table 3 lists the structural parameters obtained through analysis of the Fourier filtered EXAFS oscillations of the first coordination sphere of Ti in the samples exposed to ambient humidity. This table shows that as the zeolite hydrophilicity increases, the mean Ti−O distance becomes longer, which is usually attributed to an expansion of the coordination number,[28−31]

TABLE 1: XANES Preedge Peak Parameters for Ti−Beta Zeolites

	sample	Al/uc	Ti/uc	peak position[a] (eV)	intensity[b]	area	fwhm (eV)
Ti−Beta(F)	as-made	0	1.05	3.7	0.30	0.62	1.8
	calcined hydrated			3.8	0.68	1.22	1.6
	calcined dehydrated			3.8	1.01	1.62	1.4
Ti−Beta(OH)	calcined hydrated	0	1.63	3.9	0.42	0.87	1.9
	calcined dehydrated			3.8	0.91	1.46	1.4
Ti,Al−Beta(F)	calcined hydrated	0.54	0.73	3.8	0.66	1.19	1.5
	calcined dehydrated			3.8	0.92	1.48	1.4
Ti,Al−Beta(OH)	calcined hydrated	0.50	2.32	4.4	0.27	0.61	2.1
	calcined dehydrated			3.8	0.87	1.48	1.4

[a] Relative to the first inflection point of titanium metal (±0.2 eV). [b] Relative to the beginning of the EXAFS oscillations (±0.05).

TABLE 2: EXAFS Fitting Results for Calcined Dehydrated Samples

sample[a]	N (±0.6)	R_{Ti-O} (Å, ±0.02)	$\Delta\sigma 2$ (Å2)	ΔE_0 (eV)	fit value (10^{-3})
Ti−Beta(F)	4.2	1.79	−0.002	1.3	3.0
Ti,Al−Beta(F)	3.6	1.79	−0.002	−1.8	1.6
Ti−Beta(OH)	3.7	1.81	−0.002	0.2	1.0
Ti,Al−Beta(OH)	3.6	1.81	−0.002	1.3	1.3

[a] For Ti and Al contents, see Table 1.

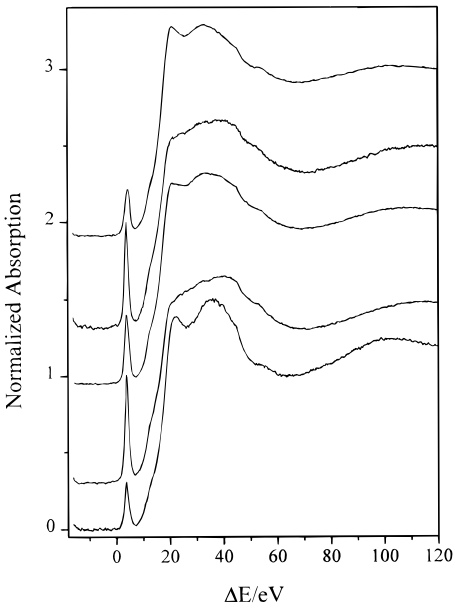

Figure 16. XANES spectra of, from bottom to top, as-made Ti−Beta-(F, 1.05 Ti/uc) and calcined rehydrated Ti−Beta(F, 1.05 Ti/uc), Ti−Beta(OH, 1.63 Ti/uc), Ti,Al−Beta(F, 0.73 Ti/uc, 0.54 Al/uc), and Ti,Al−Beta(OH, 2.32 Ti/uc, 0.50 Al/uc).

in good agreement with the XANES spectra. However, this seems to be in contradiction with the mean coordination number, as is clearly below 4 in the case of the Ti−Beta samples with longer Ti−O distances (see Table 3). We think that the anomalous low coordination value derived from EXAFS is due to the contribution of different Ti−O distances. To check this hypothesis we did a simulation of the first shell using two Ti−O bond distances. As we have discussed above, the main coordination environment of Ti in hydrated Ti−Beta(F) and Ti,Al−Beta(OH) is 5-fold and 6-fold, respectively. According to this, the simulation of the first coordination sphere of Ti considering four short and one long Ti−O bond distances for Ti−Beta(F), and four short and two long Ti−O bonds for Ti,Al−Beta(OH), led to the set of parameters collected also in Table 3. We must point out that although the bond distances seem to be quite realistic, the results obtained from the two-shell analysis must be taken with care, because many parameters are involved in the fitting. We did not carry out a similar analysis in the two other samples since the presumably increased heterogeneity of Ti sites would lead to unreliable values.

TABLE 3: EXAFS Fitting Results for Calcined Rehydrated Samples

sample[a]	N (±0.6)	R_{Ti-O} (Å, ±0.02)	$\Delta\sigma^2$ (Å^2)	ΔE_0 (eV)	fit value (10^{-3})
Ti−Beta(F)	3.6	1.81	−0.002	0.2	0.7
two-shell model[b]	4.2	1.82	−0.001	1.6	0.8
	0.7	2.12			
Ti,Al−Beta(F)	2.7	1.83	−0.004	4.8	1.6
Ti−Beta(OH)	3.1	1.86	−0.004	4.1	1.7
Ti,Al−Beta(OH)	2.6	1.85	−0.004	3.2	0.7
two-shell model[b]	4.3	1.87	0.001	4.9	8.0
	1.7	2.20			

[a] For Ti and Al contents, see Table 1. [b] For two shell-model analyses total N was constrained to be 5 and 6 for Ti−Beta(F) and Ti,Al−Beta(OH), respectively (see text).

Finally, it is also interesting to note here that the XANES spectrum of as-made Ti−Beta(F) sample presents a single peak with a low intensity and a large width (Figure 16). This peak is very similar in terms of position, intensity, area, and width to that of as-made Ti,Al−Beta(OH) previously reported.[29] The decreased intensity can be attributed to a coordination number larger than four for framework Ti. In the case of Ti,Al−Beta-(OH) samples, we proposed that framework Ti expands its coordination shell to 5 or 6 coordination by binding to one or two H_2O or OH- species, in addition to 4 framework oxygens.[29] When binding to OH^- species occurs, the negative charge introduced increases the stabilization of the framework by interaction with the template molecules. For the Beta(F) series, the spectrum of the as-made sample (Figure 16) and the changes experienced upon calcination and dehydration suggest a similar effect can also occur, though here the additional ligands can be H_2O, F^-, or OH^-.

Adsorption. One important parameter which can be expected to affect the catalytic properties of Ti-zeolites is the hydrophobicity of the material (vide infra). This is so because during the catalytic process at least two reactants with very different polar character (H_2O_2, the organic substrate, and possibly the solvent in some cases) have to reach the active sites located in the zeolitic channels, while the products formed will have to desorb and diffuse out. Thus, the ease for reactants and products to diffuse through the zeolitic channels, which strongly depends on the polar character of the zeolite, can finally determine both the activity and selectivity of the material.

To estimate the hydrophilic/hydrophobic properties of these series of materials we performed adsorption microcalorimetric experiments with three probe molecules of different polarity, H_2O, toluene, and *n*-hexane. Adsorption of *n*-hexane on pure silica Beta(F) and three Ti−Beta(F) samples with different Ti content gave identical volumetric isotherms, showing that

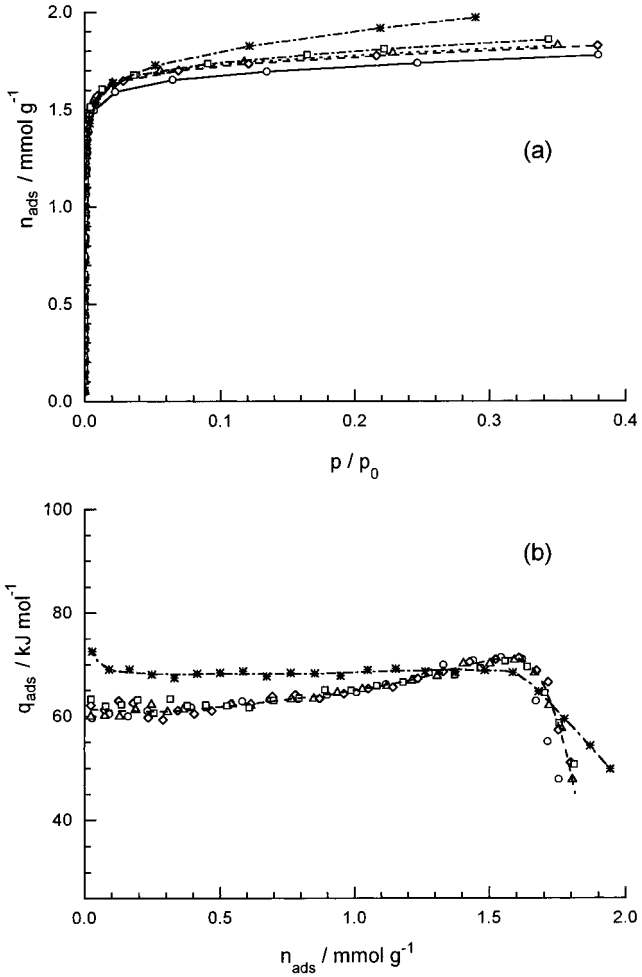

Figure 17. Volumetric (a) and calorimetric (b) isotherms of toluene adsorption on Beta samples at 315 K. Beta(F) with 0 (○), 0.68 △), 1.05 (◇), and 1.38 (□) Ti/uc and Beta(OH) with 1.11 (*) Ti/uc.

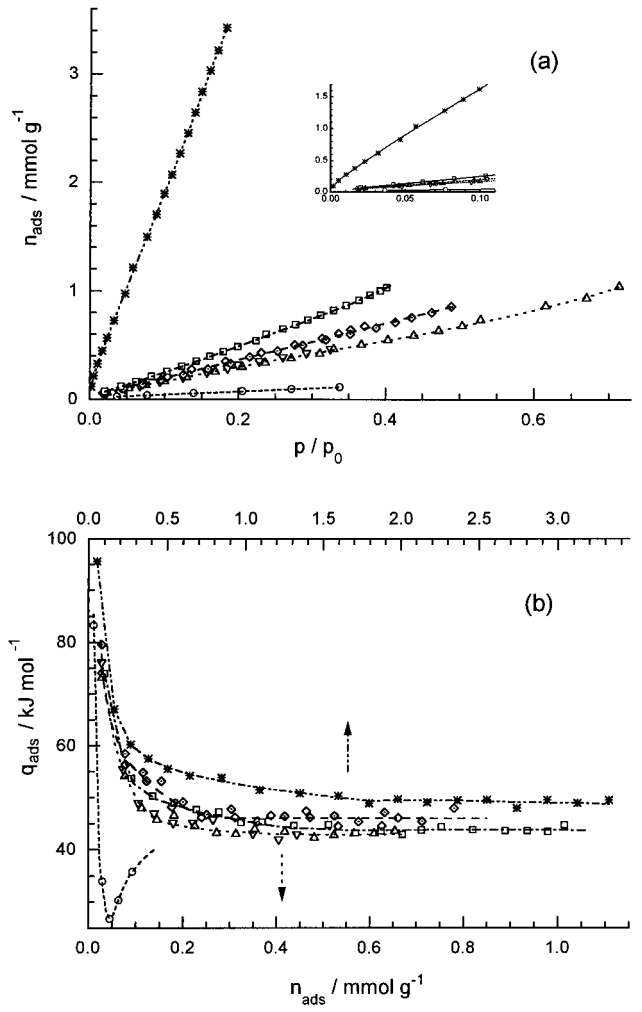

Figure 18. Volumetric (a) and calorimetric (b) isotherms of water adsorption on Ti−Beta samples at 315 K. Beta(F) with 0 (○), 0.68 (△ and ▽), 1.05 (◇), and 1.38 (□) Ti/uc and Beta(OH) with 1.11 (*) Ti/uc. Inset in (a): low relative pressure range showing that the isotherm on Ti−Beta(OH) sample belongs to type II of the BDDT classification.

incorporation of Ti does not affect the microporous volume of zeolite Beta (not shown). Furthermore, the identical calorimetric isotherms (not shown) demonstrate that there are no differences in the interaction energy between the surface of the samples and this nonpolar adsorbate. In contrast, at low coverage there is a small but nonnegligible dependence of the heat of adsorption of the more polar toluene molecule on the Ti content of the sample (Figure 17). This effect is much more apparent for the Ti−Beta(OH) sample. Additionally, Ti−Beta(F) calorimetric isotherms show an increase in the heat of adsorption as adsorption progresses, which can be attributed to adsorbate−adsorbate lateral interactions.[38] In contrast, the isotherm of Ti−Beta(OH) is characterized by a well-defined plateau, which can be explained by some specificity of the adsorption that restricts the mobility and, hence, the lateral interactions,[39] this enhanced specificity being a consequence of the much more polar character of the Ti−Beta(OH) surface.

The *n*-hexane and toluene volumetric isotherms are both characteristic of microporous solids. In contrast, water adsorption isotherms on Beta(F) samples (Figure 18a) are of type III of the BDDT classification, which is typical of water adsorption on hydrophobic surfaces. There is a linear increase of the amount of water adsorbed as the p/p_0 increases and the slope of the isotherms increases with the Ti content. The adsorption results demonstrate that, while all Beta(F) samples are essentially hydrophobic, the incorporation of Ti induces a significant increase in hydrophilicity. This effect of Ti is better evidenced when the ratio of amount of water adsorbed to amount of Ti in the zeolite is plotted against the relative pressure, the water isotherms on Ti−Beta(F) samples becoming then nearly coincident (not shown). In contrast, Ti−Beta(OH) shows an isotherm of type II (with an enhanced adsorption at low coverage) and adsorbs much larger amounts of water at any given relative pressure. This is a clear indication of the much enhanced hydrophilicity of this material.

Calorimetric isotherms of water adsorption show quite different features when pure silica Beta(F) and Ti−Beta(F) samples are compared (Figure 18b). Those obtained on the three Ti−Beta(F) present an equal profile: a steep decrease of q_{ads} with coverage that changes to a smooth decrease down to a plateau at values somewhat higher than the vaporization enthalpy of water at 315 K (ca. 43.28 kJ/mol). The plateau still continued at the end of the experiment. The extent of the decreasing part is larger the higher the Ti content of the sample is. When the isotherms are plotted as a function of the n_{ads}/n_{Ti} molar ratio, they are nearly coincident and the plateau begins at a H_2O/Ti molar ratio around or slightly over 1 (not shown). In contrast, Ti−Beta(OH) shows a much larger heat of adsorption at low coverage and the plateau begins at values higher than 3, although there is an apparent change of slope around $n_{ads}/n_{Ti} = 1$. Moreover, the heat of adsorption at the plateau is significantly higher (ca. 50 kJ mol-1) than the heat of vaporization of water.

These results suggest that while Ti−Beta(F) samples are essentially hydrophobic, the Ti centers can act as specific adsorption sites for water. The comparatively strong heterogeneous adsorption of one water molecule per titanium site is followed by weak adsorption of additional water molecules with heats of adsorption just slightly over the vaporization heat of water. This suggests that the first molecule "saturates" the Ti site and additional molecules condensate on and around the adsorption site that now consists of the first molecule adsorbed plus the Ti atom itself. In the case of Ti−Beta(OH) the interpretation of water adsorption isotherms is more difficult, because in these materials a significant contribution of the Si−OH hydrophilic moieties is expected. Nonetheless, the change of slope at n_{ads}/n_{Ti} ca. 1 indeed suggests a strong adsorption of one water molecule on each Ti site. This is followed by a less energetic adsorption which could correspond to either adsorption of a second water molecule on each Ti site or to adsorption on the Si−OH centers. In any case, for larger water uptakes the higher heat of adsorption at the plateau evidences an adsorption mechanism different from that on Ti−Beta(F), as here adsorption does not occur by mere condensation on the previously adsorbed molecules.

On the other hand, the calorimetric isotherm on the Ti-free sample (Figure 18b) exhibits a markedly different behavior, with the initial fall taking place in a very small coverage range and the adsorption heat dropping to a value well below the vaporization enthalpy and then increasing toward this enthalpy. This reflects the strict hydrophobic character of the pure silica Beta sample on which, except for a very small amount of sites (external surface defects, impurities),[40] adsorption takes place with very low adsorption heat. After reaching its minimum value, the increase in the heat of adsorption is due to cooperative adsorption, i.e., interactions with water molecules already on the surface.

Experiments of water postadsorption after toluene preadsorption were also performed (Figure 19). The isotherm on the Ti-free sample is similar to that obtained on the clean sample. However, those corresponding to Ti−Beta(F) samples are of type II of the BDDT classification. The knee at low relative pressures suggests the existence of an interaction at low water coverage stronger than that found on the bare surface. Besides that, the water uptake at a given p/p_0 increases with the Ti content, as in the clean samples.

The water postadsorption calorimetric isotherms are similar to those obtained with the clean samples, the curves that correspond to the Ti-free sample being equivalent. The heats of adsorption on Ti−Beta(F) samples are higher than those on the clean samples, especially at low coverage, and the difference is larger as the Ti content increases. In these postadsorption experiments, the uptake at which the initial descent ends and the plateau starts correlates even more clearly with the Ti content of the samples. If the adsorption heat is plotted against n_{ads}/n_{Ti} (Figure 19b), the three isotherms lie now in a single curve which defines very well the point of change at $H_2O/Ti = 1$. For the Ti−Beta(OH) sample there is a change of slope at around 1 and the plateau begins near 3−3.5.

The following description based on the analysis of the postadsorption experiments can be outlined. The amount of toluene that remains on the surface after the intermediate outgassing, calculated from the calorimetric desorption peak, is 1.18 ± 0.08 mmol g^{-1} for all the Beta(F) samples. We may speculate that toluene molecules remaining on the solids completely cover the micropores surface. The more polar water molecule would displace toluene from the Ti site and adsorb on it. The water adsorption heat is now higher than that on the bare surface because of the additional interaction of the adsorbed water molecule with toluene molecules surrounding the water/titanium centers. The total water adsorption capacity of these sites diminishes due to the presence of toluene. This makes the change from the region of heat descent to the plateau more abrupt, allowing us a more precise determination of that point and a clear demonstration of the relation between the presence of titanium and the water adsorption properties of the Ti−Beta-(F) materials.

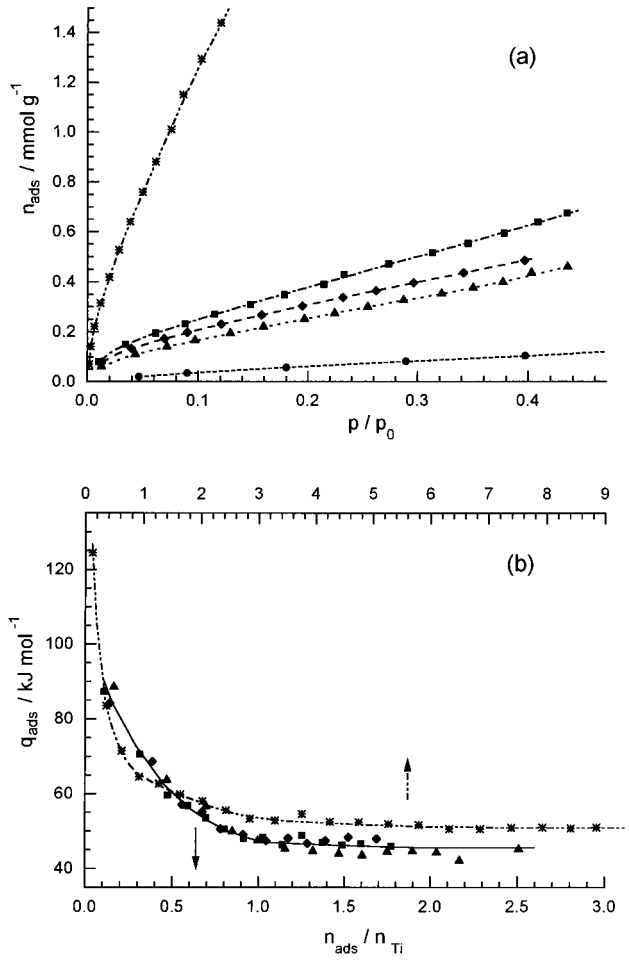

Figure 19. Volumetric (a) and calorimetric (b) isotherms of water adsorption on Ti−Beta samples at 315 K after toluene preadsorption and outgassing for 30 min at 315 K. Beta(F) with 0 (●), 0.68 (▲), 1.05 (◆), and 1.38 (■) Ti/uc and Beta(OH) with 1.11 (*) Ti/uc.

Thus, while pure SiO_2 zeolite Beta is a strictly hydrophobic material, the presence of Ti in the Ti−Beta(F) samples increases their hydrophilicity. A possible explanation for this could be the hydrolysis of Si−O−Ti bonds to give Si−OH + HO−Ti hydrophilic moieties. However, this is clearly not the case, as MAS NMR and IR experiments demonstrate that such hydrolyses do not extensively occur in Ti−Beta(F) samples (see above). Therefore, we ascribe this increase in hydrophilicity as the Ti content increases to Ti itself, which, when tetrahedrally coordinated in the zeolite framework, can expand its first coordination sphere by bonding to ligands with electron donor properties (like water and/or certain organic solvents), acting thus as a Lewis acid site. The water adsorption experiments strongly suggest that, in the case of the hydrophobic Beta(F) samples, each Ti site adsorbs one water molecule, while adsorption of successive H_2O molecules occurs by mere condensation on the water already adsorbed on the Ti sites. In contrast, Ti−Beta-

(OH) is more hydrophilic, and although there is probably a strong adsorption of one water molecule per Ti site, it is not possible from the adsorption experiments to conclude if there is adsorption of a second molecule, as suggested by the XANES results. It is clear, however, that for any water uptake considered adsorption of water on Ti−Beta(OH) is more energetic and takes place to a larger extent than on Ti−Beta(F).

From the results presented here, it appears that Ti−Beta(F) samples differ from Ti−Beta(OH) samples in three aspects: the lack of Si−OH defects, the absence of Ti−O−Si hydrolysis, and the lower coordination number of Ti upon exposure to ambient humidity. The first aspect is due to the use of F^- as mineralizer as discussed above. The second aspect is remarkable and, at a first sight, appears to be in contradiction to the conclusions of a computational calculation performed by Sinclair et al.[38] These authors concluded that tetracoordinated Ti species in zeolites would readily hydrolyze to yield Ti−OH and Si−OH species. However, their calculation showed that Ti(OSi)4 is the most stable 4-coordinated form of Ti, the energy difference of the $TiOH(OSi)_3$ + SiOH situation being about −20 kJ mol^{-1}. Only when the possibility of hydrogen bonding of the Si−OH produced to other nearby silanols or surface oxygens is considered does the difference in energy become very small (by virtue of the additional 27 kJ mol^{-1} of the hydrogen bond), and the conclusion of a likely hydrolysis is substantiated. This is most probably the case for Ti-zeolites synthesized in OH^- medium, which show a high concentration of defects, but possibly not for the defect-free Ti−Beta(F) samples. Thus, we propose the resistance to hydrolysis of Ti−O−Si bonds in Ti−Beta(F) is due to the lack of nearby Si−OH groups that could stabilize the hydrolyzed $TiOH(OSi)_3$ + SiOH situation by hydrogen bonding to the silanol produced. Once this particular feature of Ti−Beta(F) has been proved, the third aspect above can be easily understood: a restricted flexibility of the unhydrolyzed $Ti(OSi)_4$ species compared to the hydrolyzed $TiOH(OSi)_3$ groups can be expected; consequently, $Ti(OSi)_4$ species (predominant in Ti−Beta(F)) would be less able to accommodate more than one additional H_2O molecule in its first coordination sphere. A loose coordination at a rather long distance of one water molecule to the Ti site in Ti−Beta(F) with just a slight distortion of its tetrahedral geometry (with a small increase in length of the four Ti−O bonds to the framework) can explain the XANES results. Unfortunately, the Ti content in these samples is not large enough to allow a precise EXAFS analysis assuming a 4+1 or 4+2 coordination shells with very long distances to water. However, comparison with the results obtained for the Ti−Beta(OH) sample (larger increase in Ti−O distances and enhanced broadening and decreased intensity of the prepeak) suggests that in Ti−Beta(OH) rehydration forces Ti to adopt a geometry in which the distance to water molecules are shorter and then those to zeolitic O are larger than in Beta(F); that is in the material prone to hydrolysis of Si−O−Ti bonds Ti reaches a larger coordination shell upon hydration. Finally, we note here that this discussion holds for zeolites exposed to ambient humidity or to water vapor, while the typical conditions for oxidation reactions, i.e., the presence of H_2O_2, could likely force a completely different scenario. Effectively, the large affinity of H_2O_2 for Ti could possibly favor the hydrolysis of Ti−O−Si bonds in Ti-Beta(F) during the catalytic reaction.

Catalytic Activity and Selectivity. Results of the catalytic epoxidation of 1-hexene with H_2O_2 using Ti−Beta(F) in two solvents, acetonitrile and methanol, are compared in Table 4 with those obtained using Ti−Beta(OH) and TS-1. Ti−Beta synthesized in F^- medium is an active oxidation catalyst, as expected from the characterization results that indicate the isomorphous replacement of Si by Ti in the framework (see above). Moreover, the activity of Ti−Beta(F) is seen to be higher in acetonitrile than in methanol, as opposed to TS-1 and as found earlier also for Ti−Beta(OH).[4] The higher performance of Ti−Beta(OH) over TS-1 in acetonitrile was early attributed to the more hydrophilic character of Ti−Beta(OH). However, the results shown in Table 4 demonstrate that hydrophobic Ti−Beta(F) (see above) behaves in a similar way. Therefore, the difference between TS-1 and Ti−Beta catalysts in different solvents appears to be somehow "intrinsic" to the zeolitic structure rather than being related to the surface physicochemical properties of the materials.

TABLE 4: Epoxidation of 1-Hexene over Ti-Containing Zeolites[a]

catalyst	TiO_2 (wt %)	solvent	1-hexene conversion[b]	epoxide selectivity	H_2O_2 selectivity	TON[c]
Ti−Beta(F)	2.86	CH_3CN	41.2	100	99.7	43.1
Ti−Beta(OH)	2.78	CH_3CN	40.3	100	76.6	53.4
TS-1	2.18	CH_3CN	25.5	100	76.5	39.1
Ti−Beta(F)	2.86	CH_3OH	26.8	76.6	97.9	30.7
Ti−Beta(OH)	2.78	CH_3OH	25.4	54.9	90.1	24.2
TS-1	2.18	CH_3OH	46.6	97.6	96.7	94.5

[a] Reaction conditions: 16.5 mmol 1-hexene, 11.8 g solvent, 4.1 mmol H_2O_2, 100 mg catalyst, 50 °C, 2h. [b] Percentage of maximum. [c] initial turnover number (moles of converted olefin/moles of Ti × hours).

Ti−Beta(F) and Ti−Beta(OH) show similar activities in both solvents, although the difference in initial turnovers is not negligible: Ti−Beta(F) is more active than Ti−Beta(OH) in methanol, while the opposite is true in acetonitrile. The most significant differences between Ti−Beta catalysts synthesized in F^- and OH- media refer to their selectivities. While the selectivity to the epoxide in acetonitrile is always very high regardless of the zeolite, in methanol Ti−Beta(F) is more selective than Ti−Beta(OH). Both Ti−Beta samples are however less selective than TS-1 in methanol. The relatively low selectivity in methanol of Ti−Beta catalysts when compared to TS-1 catalysts was early attributed to the presence of acid sites in Ti,Al−Beta(OH).[5] Actually, when new synthetic methods allowed the increase of the Si/Al ratio to values as high as 700, the selectivity of Ti,Al−Beta(OH) was shown to increase.[7] However, the synthesis of Al-free Ti−Beta in OH^- medium proved that even in the complete absence of Al the oxirane ring was still opened to some extent.[8] The lower selectivity of Ti−Beta to the epoxide when compared to TS-1 was then attributed to the intrinsic higher acidity of Ti sites in the zeolite Beta structure. However, an effect of the hydrophilic character of Ti−Beta(OH) on the selectivity (through an enhanced adsorption of the epoxide formed on the Ti sites of zeolite Beta) could not be discarded.[8] The results presented in Table 4 demonstrate that, while the adsorption properties of Ti−Beta actually play a significant role in its selectivity to the epoxide, the differences with TS-1 are predominantly "intrinsic" and, thus, may be attributed to a stronger acidity of Ti or Ti−H_2O_2 sites in the Beta structure. Additionally, the selectivity of Ti−Beta(F) in the use of H_2O_2 is very high in either solvent, while both Ti−Beta(OH) and TS-1 are markedly less selective in acetonitrile.

Finally, the differences in surface properties between Ti−Beta(OH) and Ti−Beta(F) are more critical when the substrate to be oxidized contains a polar moiety. As shown in Table 5, Ti−Beta(F) is more active in the epoxidation of oleic acid than Ti−Beta(OH) and makes more efficient use of H_2O_2. We found similar results in the epoxidation of methyl oleate.[9] These

TABLE 5: Epoxidation of Oleic Acid over Ti−Beta Zeolites[a]

catalyst	TiO_2 (wt %)	acid conversion[b]	epoxide selectivity	H_2O_2 selectivity
Ti−Beta(F)	2.52	31.2	100	67.6
Ti−Beta(OH)	2.78	20.2	100	24.8

[a] Reaction conditions: 1 mmol oleic acid, 2 mL CH_3CN, 0.25 mmol H_2O_2, 30 mg catalyst, 50 °C, 8 h. [b] Percentage of maximum.

differences may be attributed to the different adsorption properties of both catalysts, as in Ti−Beta(OH) a strong adsorption of oleic acid through the polar head would make more difficult the oxidation of the double bond in the middle of the hydrocarbon chain.

Conclusions

The feasibility of Ti incorporation into the framework of both pure silica and aluminosilicate zeolite Beta in fluoride medium has been demonstrated by the combination of powder X-ray diffraction, adsorption and spectroscopic techniques, and catalytic testing. FTIR, ^{29}Si MAS NMR, and ^{1}H→^{29}Si CP MAS NMR spectroscopies demonstrate a fundamental difference between Beta materials synthesized in fluoride and in OH^- media: the lack of Si−OH connectivity defects in Beta(F) samples as opposed to the very high concentration of such defects in Beta(OH) samples. In Beta(F) only Si−OH moieties ascribed to terminal groups in the external surface of the crystallites exist. There is no dependence of the Si−OH concentration on the Ti content of the sample, suggesting that the hydrolysis of Si−O−Ti bonds, if any, does not occur to a large extent. However, this can be a major feature of Ti−Beta-(OH) samples.

This difference in Si−OH concentration determines the different polar character of the materials synthesized in F^- and OH^- media, which has been clearly demonstrated by means of microcalorimetric adsorption experiments. While pure SiO_2 zeolite Beta is a material strictly hydrophobic, the presence of Ti in the Ti−Beta(F) samples increases their hydrophilicity. The enhanced hydrophilicity is due to Ti itself which, when tetrahedral in the zeolite framework, can expand its first coordination sphere by bonding to ligands with electron donor properties (like water and/or certain organic solvents), acting thus as a Lewis acid site. The water adsorption experiments strongly suggest that, in the case of the hydrophobic Ti−Beta-(F) samples, each Ti site strongly adsorbs one water molecule, while adsorption of successive H_2O molecules occurs by mere condensation on the water already adsorbed on the Ti sites. According to the XANES and adsorption experiments, in the Beta(OH) series possibly more than one water molecule could be adsorbed on each Ti site. We propose that this difference between Beta(F) and Beta(OH) materials is a consequence of the resistance to hydrolysis of the Ti−O−Si bonds in Ti−Beta-(F), which restricts the flexibility of the Ti center.

Finally, the catalytic activity and selectivity of Ti−Beta(F) samples are qualitatively similar to those of Ti−Beta(OH), and this can be regarded as a further support of the isomorphous substitution. Moreover, when the activity and selectivity of the Beta(F) and Beta(OH) series are compared in different solvents, the same trends are observed. Notably, their activity and selectivity in the epoxidation of alkenes is higher in acetonitrile than in methanol, contrarily to the observations made with TS-1. Therefore, this is a peculiarity of Ti−Beta materials, and it is not due to the presence of acid centers in Al−(OH)−Si bridges or to the hydrophilic properties of the samples. Furthermore, the differences in selectivity between TS-1 and Ti−Beta materials in the epoxidation of alkenes are also, to a considerable extent, "intrinsic" to these zeolitic structures: the opening of the oxirane ring in protic solvents is catalyzed, though to different extents, by all classes of Ti−Beta materials, and this is not only due to acidity related to residual Al in the samples nor is it simply favored by an enhanced hydrophilicity of the materials. It is probably an enhanced acidity of the Ti (or Ti−H_2O_2) sites in the Beta structure that accounts for the difference with TS-1 in the selectivity to the epoxide. On the other hand, the enhanced hydrophobicity of Ti−Beta(F) materials can determine their activity and selectivity, especially in the oxidation of organic substrates containing a polar moiety.

Acknowledgment. The authors gratefully acknowledge the Spanish DGICYT (UR95-0075, UR1995-0192-01 and MAT 94-0359-C02-01), and the EEC Human Capital and Mobility Program for financial support, Dr. F. Rey (ITQ) and Dr. F. Villain and Dr. R. Cortes (LURE, Orsay) for help in collecting the XAFS spectra, the Comité de Programme of LURE for allocating data collection time in the XAS-2 and XAS-3 stations, and Dr. Cefe López (ICM, Madrid) for the micro-Raman measurements. P.E. gratefully acknowledge the Generalitat Valenciana for a postgraduate scholarship.

References and Notes

(1) Sheldon, R. A. *J. Mol. Catal.* **1980**, *7*, 107.
(2) Taramasso, M.; Perego, G.; Notari, B. U.S. Patent 4,410,501, 1983.
(3) Camblor, M. A.; Corma, A.; Martínez, A.; Pérez-Pariente, J. *J. Chem. Soc., Chem. Commun.* **1992**, 589.
(4) Corma, A.; Esteve, P.; Martínez, A. *J. Catal.* **1996**, *161*, 11.
(5) Corma, A.; Camblor, M. A.; Esteve, P.; Martínez, A.; Pérez-Pariente, J. *J. Catal.* **1994**, *145*, 151.
(6) Camblor, M. A.; Corma, A.; Martínez, A.; Pérez-Pariente, J.; Valencia, S. *Stud. Surf. Sci. Catal.* **1994**, *82*, 531.
(7) Camblor, M. A.; Costantini, M.; Corma, A.; Esteve, P.; Gilbert, L.; Martínez, A.; Valencia, S. In *The Roots of Organic Development*; Desmurs, J. R., Ratton, S., Eds.; Elsevier: Amsterdam, 1996, p 391.
(8) Camblor, M. A.; Costantini, M.; Corma, A.; Gilbert, L.; Esteve, P.; Martínez A.; Valencia, S. *Chem. Commun.* **1996**, 1339.
(9) Blasco, T.; Camblor, M. A.; Corma, A.; Esteve, P.; Martínez, A.; Prieto, C.; Valencia, S. *Chem. Commun.* **1996**, 2367.
(10) Camblor, M. A.; Corma, A.; Pérez-Pariente, J. *Zeolites* **1993**, *13*, 82.
(11) Camblor, M. A.; Corma, A.; Mifsud, A.; Pérez-Pariente, J.; Valencia, S. *Stud. Surf. Sci. Catal.* **1997**, *105*, 341.
(12) Bourgeat-Lami, E.; Fajula, F.; Anglerot, D.; Des Courieres, T. *Microporous Mater.* **1993**, *1*, 237.
(13) (a) Michalowicz, A. *Logiciels pour la Chimie;* Societé Francaise de Chimie: Paris, 1991; pp 116-117. (b) Noinville, V.; Michalowicz, A.; Galaad. *Ibid*. pp 148-149.
(14) Mckale, A. G.; Veal, B. W.; Paulikas, A. P.; Chan, S. K.; Knapp, G. S. *J. Am. Chem. Soc.* **1988**, *110*, 3763.
(15) (a) Thamm, H. *Zeolites* **1987**, *7*, 341. (b) Jänchen, J.; Stach, H.; Grobet, P. J.; Martens, J. A.; Jacobs, P. A. *Zeolites* **1992**, *12*, 9.
(16) Camblor, M. A.; Hong, S. B.; Davis, M. E. *Chem. Commun.* **1996**, 425.
(17) (a) Newsam, J.M; Treacy, M. M. J.; Koetsier, W. T.; de Gruyter, C. B. *Proc. R. Soc. London A* **1988**, *420*, 375. (b) Higgins, J. B.; LaPierre, R. B.; Schlenker, J. L.; Rohrman, A. C.; Wood, J. D.; Kerr G. T.; Rohrbaugh, W. J. *Zeolites* **1988**, *8*, 446.
(18) Camblor, M. A.; Corma, A.; Valencia, S. *Chem. Commun.* **1996**, 2365.
(19) Perego, G.; Bellussi, G.; Corno, C.; Taramasso, M.; Buonomo, F.; Esposito, A. *Stud. Surf. Sci. Catal.* **1986**, *28*, 129.
(20) Gabelica, Z.; Guth, J. L. *Stud. Surf. Sci. Catal.* **1989**, *49*, 421.
(21) Iler, R. K. *The Chemistry of Silica*; Wiley: New York, 1979.
(22) Koller, H.; Lobo, R. F.; Burkett, S. L.; Davis, M. E. *J. Phys. Chem.* **1995**, *99*, 12588.
(23) Boccuti, M. R.; Rao, K. M.; Zecchina, A.; Leofanti, G.; Petrini, G. *Stud. Surf. Sci. Catal.* **1989**, *48*, 133.
(24) Huybrechts, D. R. C.; Buskens, Ph. L.; Jacobs, P. A. *J. Mol. Catal.* **1992**, *71*, 129.

(25) Camblor, M. A.; Corma, A.; Pérez-Pariente, J. *J. Chem. Soc., Chem. Commun.* **1993**, 557.

(26) (a) Rao, P. R. H. P.; Ramaswamy, A. V. *J. Chem. Soc., Chem. Commun.* **1992**, 1245. (b) Chapus, T.; Tuel, A.; Ben Taarit, Y.; Naccache, C. *Zeolites* **1994**, *14*, 349. (c) Mal, N. K.; Ramaswamy, V.; Rakshe, B.; Ramaswamy, A. V. *Stud. Surf. Sci. Catal.* **1997**, *105*, 357.

(27) Bellussi, G.; Rigutto, M. S. *Stud. Surf. Sci. Catal.* **1994**, *85*, 177.

(28) (a) Lopez, A.; Kessler, H.; Guth, J. L.; Tuilier, M. H.; Popa, J. M. *Procedings 6th Int. Conf. X-ray Absorption Fine Structure*; Hasnain, S. S., Ed., Ellis Horwood: New York, 1991, p 549. (b) Lopez, A.; Tuilier, M. H.; Guth J. L.; Delmotte, L.; Popa, J. M. *J. Solid State Chem.* **1993**, *102*, 480. (c) Trong On, D.; Bonneviot, L.; Bittar, A.; Sayari, A.; Kaliaguine, S. *J. Mol. Catal.* **1992**, *74*, 233. (d) Reddy, K. M.; Kaliaguine, S.; Sayari, A.; Ramaswamy, A. V.; Reddy, V. S.; Bonneviot, L. *Catal. Lett.* **1994**, *23*, 175.

(29) Blasco, T.; Camblor, M. A.; Corma, A.; Perez-Pariente, J. *J. Am. Chem. Soc.* **1993**, *115*, 11806.

(30) Bordiga, S.; Coluccia, S.; Lamberti, C.; Marchese, L.; Zecchina, A.; Boscherini, F.; Buffa, F.; Genoni, F.; Leofanti, G.; Petrini, G.; Vlaic, G. *J. Phys. Chem.* **1994**, *98*, 4125.

(31) Davis, R. J.; Liu, Z.; Tabora, J. E.; Wieland, W. S. *Catal. Lett.* **1995**, *34*, 101.

(32) (a) Yarker, C. A.; Johnson, P. A. V.; Wright, A. C.; Wong, J.; Greegor, R. B.; Lytle, F. W.; Sinclair, R. N. *J. Non-Cryst. Solids* **1986**, *79*, 117; (b) Waychunas, G. A. *Am. Mineral.* **1987**, *72*, 89.

(33) Behrens, P.; Felsche, J.; Vetter, S.; Schulz-Ekloff, G.; Jaeger, N. I.; Niemann, W. *J. Chem. Soc., Chem. Commun.* **1991**, 678.

(34) Greegor, R. B.; Lytle, F. W.; Sandstrom, D. R.; Wong, J.; Schultz, P. *J. Non-Cryst. Solids* **1983**, *55*, 27.

(35) (a) Wu, K.; Brown, I. D. *Acta Crystallogr.* **1973**, *B 29*, 2009. (b) Babonneau, F.; Doeuff, S.; Leaustic, A.; Sanchez, C.; Cartier, C.; Verdaguer, M. *Inorg. Chem.* **1988**, *27*, 3166.

(36) Pei, S.; Zajac, G. W.; Kaduk, J. A.; Faber, J.; Boyanov, B. I.; Duck, D.; Fazzini, D.; Morrison, T. I.; Yang, D. S. *Catal. Lett.* **1993**, *21*, 333.

(37) Le Noc, L.; Trong On, D.; Solomykina, S.; Echchahed, B.; Béland, F.; Cartier dit Moulin, C.; Bonneviot, L. *Stud. Surf. Sci. Catal.* **1996**, *101*, 611.

(38) Sinclair, P. E.; Sankar, G.; Catlow, C. R. A.; Thomas, J. M.; Maschmeyer, T. *J. Phys. Chem. B* **1997**, *101*, 4232.

(39) Corma, A.; Corell, C.; Pérez-Pariente, J.; Guil, J. M.; Guil-López, R.; Nicolopoulos, S.; González-Calvet, J.; Vallet-Regí, M. *Zeolites* **1996**, *16*, 7.

(40) Gregg, S. J.; Sing, K. S. W. *Adsorption, Surface Area and Porosity*, Academic Press, London, 1982; Chapter 5.